Pollutant Transport and Diffusion in Katabatic Flows

CARMEN J. NAPPO, K. SHANKAR RAO AND JEROLD A. HERWEHE*

Atmospheric Turbulence and Diffusion Division, NOAA/ARL, Oak Ridge, Tennessee

(Manuscript received 17 February 1988, in final form 24 June 1988)

ABSTRACT

The characteristics of pollutant transport and diffusion of a passive contaminant in a two-dimensional katabatic flow over a simple slope are examined using a primitive equation hydrodynamic model. It is shown that pollutants released above the drainage layer can be entrained into the layer and diffused to the ground surface. For elevated releases within the drainage layer, subsidence in the flow leads to relatively high surface concentrations of pollutants close to the stack. Pollutants released at ground level can spread through the entire depth of the drainage layer. This vertical diffusion is more effective for a shallow slope, resulting in higher concentrations at all heights, than for a steeper slope. These dispersion characteristics are quite different from those for stable flows over flat terrain. The differences result from increases of boundary-layer depth, wind speed, and turbulence as the katabatic flow develops downslope.

The katabatic flow and dispersion model is tested by simulating the perfluorocarbon and heavy methane tracer releases for Night 4 of the 1980 ASCOT field study in Anderson Creek Valley, California. These tests show that the observed concentrations and the depth of the drainage layer in the lower region of the slope are underpredicted because the model could not simulate the convergence of drainage air (pooling) in the valley basin. The nightly average values of the observed concentrations, however, are predicted well. It is concluded that the model is applicable to nearly two-dimensional open slopes.

1. Introduction

An important element of the U.S. Department of Energy's Atmospheric Studies in Complex Terrain (ASCOT) program is the development of models for transport and diffusion in nocturnal drainage flows. In this paper, we study the diffusion in a flow over sloping terrain under stable conditions. Dispersion in this katabatic flow is quite different from dispersion in a stable boundary layer (SBL) flow over flat terrain. In the latter case, since vertical dispersion above the SBL is negligible, pollutants released there tend to remain at that level until they are entrained into the growing mixed layer next morning. Pollutants released above the katabatic layer, however, may be entrained into the drainage flow if the slope is long enough, and are rapidly diffused to the ground. Since this process cannot be accounted for in standard Gaussian plume and puff models, such models can be expected to underestimate ground-level concentrations far downslope from the source.

The need to model the details of the dynamics of drainage flows was recognized early in the ASCOT program. Over flat terrain, the SBL depth, the pollutant transport wind, and the rate of vertical dispersion near the source can all be considered constant with horizontal distance, but in a katabatic flow these variables will be functions of downslope distance. The laboratory investigations of Ellison and Turner (1959) and the linear analyses of Briggs (1981), which were restricted to neutral ambient thermal stratification and negligible winds aloft, predict a linear growth of katabatic layer thickness with downslope distance. If, for simplicity, it is assumed that pollutants are uniformly mixed through the depth of the drainage layer, then one would predict pollutant concentrations to decrease continuously with downslope distance in this type of flow. Subsequently, using the complete nonlinear governing equations for katabatic flows over uniform simple slopes, Nappo and Rao (1987) demonstrated that the drainage layer thickness and velocity approach constant values with downslope distance, and the entrainment rate vanishes for critical values of slope angle, downslope distance, and ambient thermal stratification. These characteristics strongly influence the dispersion of pollutants in a drainage flow because when entrainment ceases and the layer depth becomes constant, dilution occurs only through the lateral spread of the material. Generally, one can expect entrainment rate to decrease with downslope distance, so that dilution rate also decreases with distance from the source. This behavior cannot be accounted for in standard dispersion modeling techniques which assume constant dif-

* Oak Ridge Associated Universities, Oak Ridge, TN. On permanent assignment to ATDD.

Corresponding author address: Dr. Carmen J. Nappo, ATDD, NOAA/ARL, P.O. Box 2456, Oak Ridge, TN 37831.

Unauthenticated | Downloaded 05/21/24 07:09 AM UTC

fusivities. This limitation of standard dispersion modeling techniques in predicting pollutant concentrations in buoyancy-driven slope flows has been observed by Willson et al. (1983) and King et al. (1987). From field studies, they concluded that dispersion in these flows is strongly influenced by the entrainment, and growth of the boundary layer.

In this paper, we illustrate some of the basic characteristics of transport and diffusion of pollutants in katabatic flows using a two-dimensional primitive equation model, and demonstrate the utility of this model for predicting concentrations over slopes which are only approximately two-dimensional. Specifically, we examine the downslope variations of pollutant concentrations as functions of the ratios of release height, H, to local drainage layer depth, h, for 2.5° and 20° slopes, and simulate some of the tracer tests performed during Night 4 of the 1980 ASCOT field study in Anderson Creek Valley in the Geysers area of northern California. Our results show that the concentration patterns are substantially different from those given by Gaussian plume formulae, and this difference can be attributed to the entrainment of ambient air into the drainage layer and the downslope variations of wind speed and turbulence.

2. The model

The model used in this study is that described in Nappo and Rao (1987), with the addition of the species-conservation equation,

$$\frac{\partial C}{\partial t} + u\frac{\partial C}{\partial s} + w\frac{\partial C}{\partial n} = \frac{\partial}{\partial n}\left(K_h\frac{\partial C}{\partial n}\right), \qquad (1)$$

where C is the concentration of the pollutant and K_h is the eddy diffusivity for heat (and mass). The open slope is assumed to be two-dimensional with uniform surface characteristics. The (s, y, n) coordinate system, with its origin at the crest of the slope, is aligned such that the s-axis is along the fall-line, and the n-axis is normal to the slope. The u and w velocity components are in the s and n-directions, respectively. The computational grid has uniform spacing along the s-axis and logarithmic spacing along the n-axis. The domain of the grid is 3000 m × 600 m with 31 × 31 points. The model is initialized as described in Nappo and Rao (1987).

Turbulence is parameterized in terms of e, the turbulent kinetic energy (TKE), which is directly calculated in the model. At the inflow boundary, located at the ridge crest, all variables are held constant at their ambient values; at the outflow boundary, we require the downslope gradients of the variables to be zero. At the ground surface, fluxes of heat and momentum normal to the surface are calculated from flux-profile relations (Businger et al. 1971) based on local similarity assumptions. The eddy diffusivity K_h is calculated from

$$K_h = l_h(0.2e)^{1/2}, \qquad (2)$$

where l_h is the turbulent mixing length given by

$$l_h = \frac{kn}{0.74 + 4.7\left(\frac{n - z_0}{L}\right)}, \qquad (3)$$

where k is the von Kármán constant, z_0 is the surface roughness, and L is the Monin–Obukhov length.

For pollutants, we assume a perfectly reflecting surface, i.e., the flux of pollutants near the ground is set equal to zero. Because the model is two-dimensional, the source is an infinite cross-wind line source located at $s = s_0$ and $n = H$. At $s = s_i > s_0$, we specify an initial concentration profile (which serves as the inflow boundary condition) using the Gaussian plume formula for a line source:

$$C(s_i, n) = \frac{Q}{\sqrt{2\pi}u\sigma_n}\left\{\exp\left[-\frac{(n-H)^2}{2\sigma_n^2}\right] + \exp\left[-\frac{(n+H)^2}{2\sigma_n^2}\right]\right\} \qquad (4)$$

where

$$\sigma_n = 2K_h(s_i - s_0)/u, \qquad (5)$$

with u and K_h values calculated at (s_0, H), and Q is the line source emission rate. This initialization for the concentration field is necessary since the numerical grid cannot resolve the plume until it grows large enough to be described by the finite difference scheme, i.e., $\sigma_n > \Delta n$. The development of the concentration profiles downslope, away from the vicinity of the source, is not very sensitive to the assumed initial concentration profile; therefore, the latter can be specified by any realistic distribution $C_i(n)$ which satisfies the integral mass conservation equation

$$\int_0^\infty C_i u dn = Q. \qquad (6)$$

3. Dispersion characteristics

To illustrate the effects of slope angle and source height on dispersion in katabatic flows, a series of computer runs were made for slope angles of 2.5° and 20°, and H/h values of 0, 0.5, 1, and 2. For all runs, the following conditions were specified: total surface cooling of 4°C, ambient thermal stratification of 6°C km^{-1}, ambient wind speed of 3 m s^{-1} in the downslope direction, surface roughness of 0.10 m, and source location s_0 = 300 m. Numerical integrations were carried out to t = 4 hours to ensure the establishment of a steady state.

Figure 1 shows the vertical profiles of drainage velocity at various distances from the crest of the slope for the two slope angles. The speed and the height of the jet increase with downslope distance. For the steeper slope, the development of the jet is more pronounced,

Unauthenticated | Downloaded 05/21/24 07:09 AM UTC

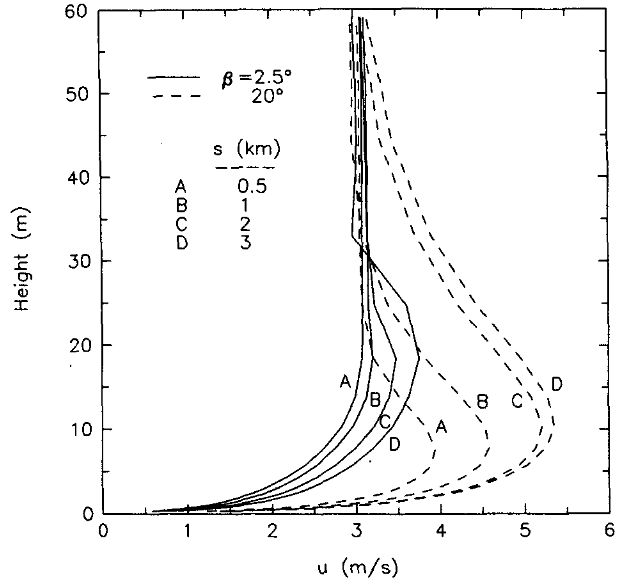

FIG. 1. Mean velocity profiles at several downslope distances, s, in the katabatic flow over 2.5° and 20° slopes. The ambient wind is 3 m s^{-1} downslope.

with a significantly larger speed at a smaller height, than for the shallow slope. Figures 2a and 2b show the corresponding eddy diffusivity profiles computed by the model for the two slope angles. It can be seen that the turbulent kinetic energy, and hence K_h, increase with the downslope distance, with much larger values for the steeper slope. This characteristic of the katabatic flows accounts for entraining the elevated plume material into the flow and bringing it down to the ground-level, as discussed below.

Isopleths of $(C/Q) \times 10^3$ are plotted in Figs. 3 and 4 for slope angles of 2.5° and 20°, respectively, for $H/h = 2, 0.5$, and 0, where $h = h(s_0)$ is the local drainage layer depth. The variation of $h(s)$, determined as the height where the TKE decreases to 1% of its local maximum value, is also shown in the figures. This definition of h is somewhat arbitrary and, from the eddy diffusivity profiles (Fig. 2), it can be seen that significant levels of turbulence exist above $h(s)$; therefore, the scale height h cannot be considered as the height of a lid limiting vertical diffusion.

The transport of pollutants toward the ground surface by subsidence is clearly illustrated in Figs. 3a and 4a for releases of pollutants above the drainage layer. The mean subsidence velocity, w, is calculated at each level in the model by integrating the mass continuity equation from the ground surface up to that level. Profiles of w at various downslope distances for the 20° slope are shown in Fig. 5. Subsidence increases almost linearly from zero at the ground surface to a maximum value at the top of the drainage layer. Below 100 m height, w attains a maximum value of about 3.5 cm s^{-1} at about $s = 1$ km, and then rapidly decreases with increasing s. Thus the downward tilt of the pollutant plume decreases with increasing downslope distance as shown in Figs. 3a and 4a. The entrainment and settling of the elevated plume by subsidence is an important property of katabatic flows, which distinguishes it from the behavior of the plume released above the SBL over flat terrain.

Figures 3b and 4b illustrate the effects of drainage wind speed on the plume dispersion for the case of $H/h = 0.5$. The pollutant is released above the drainage jet, which is located at a height of about $0.25h$ for this case. As both the height and speed of the jet initially increase with s (see Fig. 1), however, the pollutants

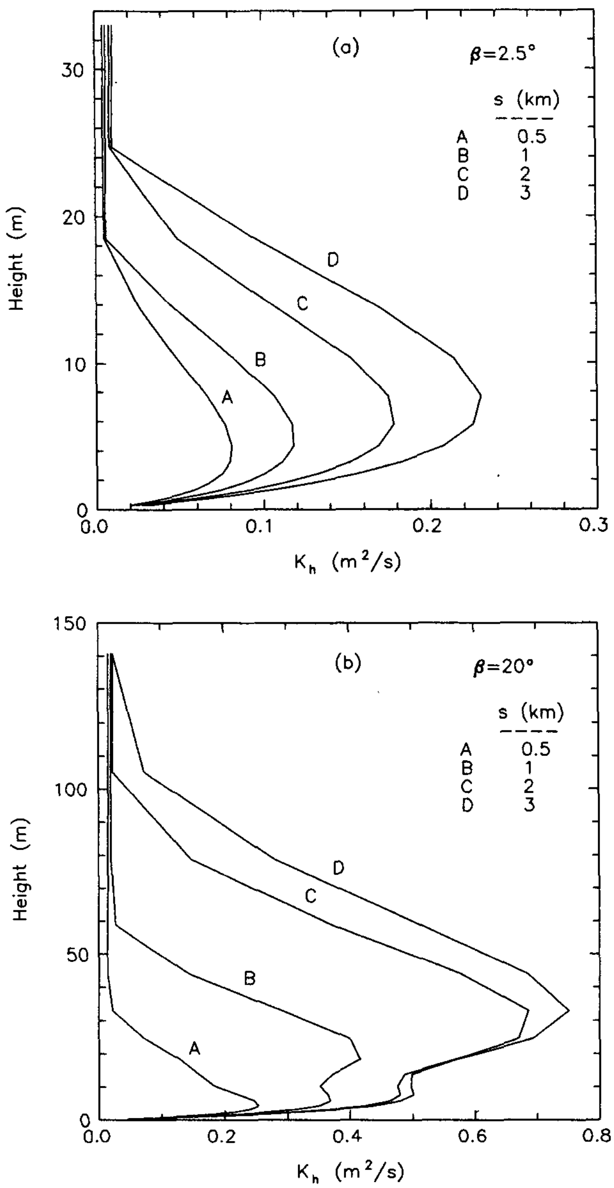

FIG. 2. Vertical profiles of eddy diffusivity, K_h, at several downslope distances, s, in the katabatic flow. (a) $\beta = 2.5°$, and (b) $\beta = 20°$.

Unauthenticated | Downloaded 05/21/24 07:09 AM UTC

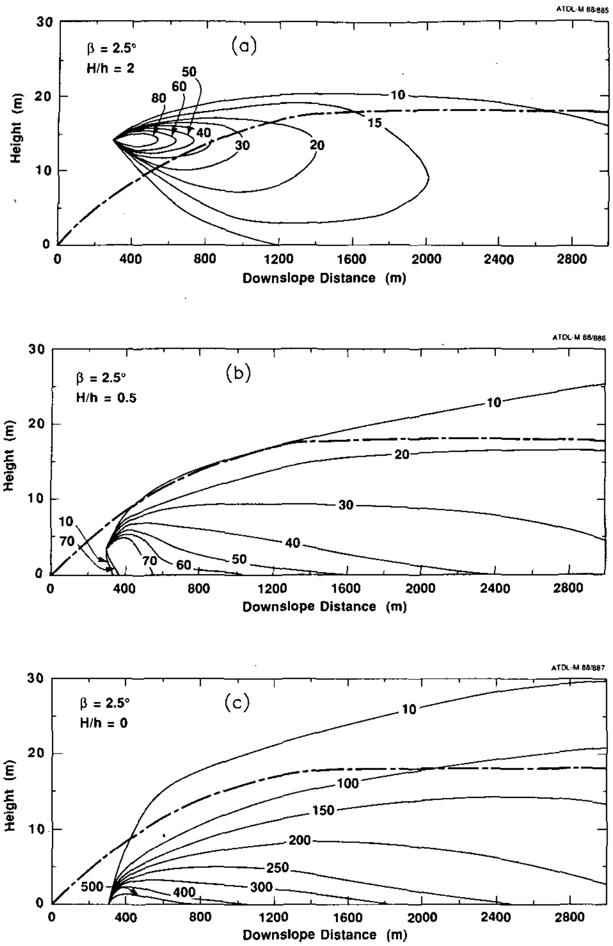

FIG. 3. Isopleths of $(C/Q) \times 10^3$ s m^{-2} above the 2.5° slope for different values of the ratio of source height, H, to the local drainage layer depth, h. The latter, indicated by a heavy broken line, is smaller than the height to which turbulence extends in the flow. See text for details. (a) $H/h = 2$, (b) $H/h = 0.5$, and (c) $H/h = 0$.

are advected downslope with increasing speed, leading to the low values of C/Q at stack heights. The sharp downward tilt of the plume near the release point in Figs. 3b and 4b illustrates the importance of subsidence within the drainage flow in bringing high concentrations of pollutants to the ground-level very close to the stack location. In an analysis of the 1984 Brush Creek tracer data, Rao et al. (1989) noted that relatively high concentrations were observed at ground-level samplers located on two arcs near the site of an elevated release within the Brush Creek drainage, and attributed these high concentrations to the occurrence of strong subsidence in the flow.

The isopleths for the surface releases shown in Figs. 3c and 4c also reflect the effects of the difference in wind speed over the two slopes. Nappo and Rao (1987) showed that drainage wind speed increases with slope angle. The low wind speeds over the 2.5° slope (see Fig. 1) allow the pollutants to build up and establish large vertical gradients near the ground. The resulting upward turbulent transfer of pollutants significantly exceeds their downward transport by subsidence. Over the 20° slope, the wind speeds are greater than over the 2.5° slope and, consequently, the surface concentrations and their vertical gradients are not as large. In Figs. 3b and 3c, it should be noted that the upper edge of the plume (denoted by the isopleth marked 10) extends above $h(s)$ because, as discussed earlier, the drainage layer depth h (as defined in this study) is smaller than the height to which turbulence extends in the flow.

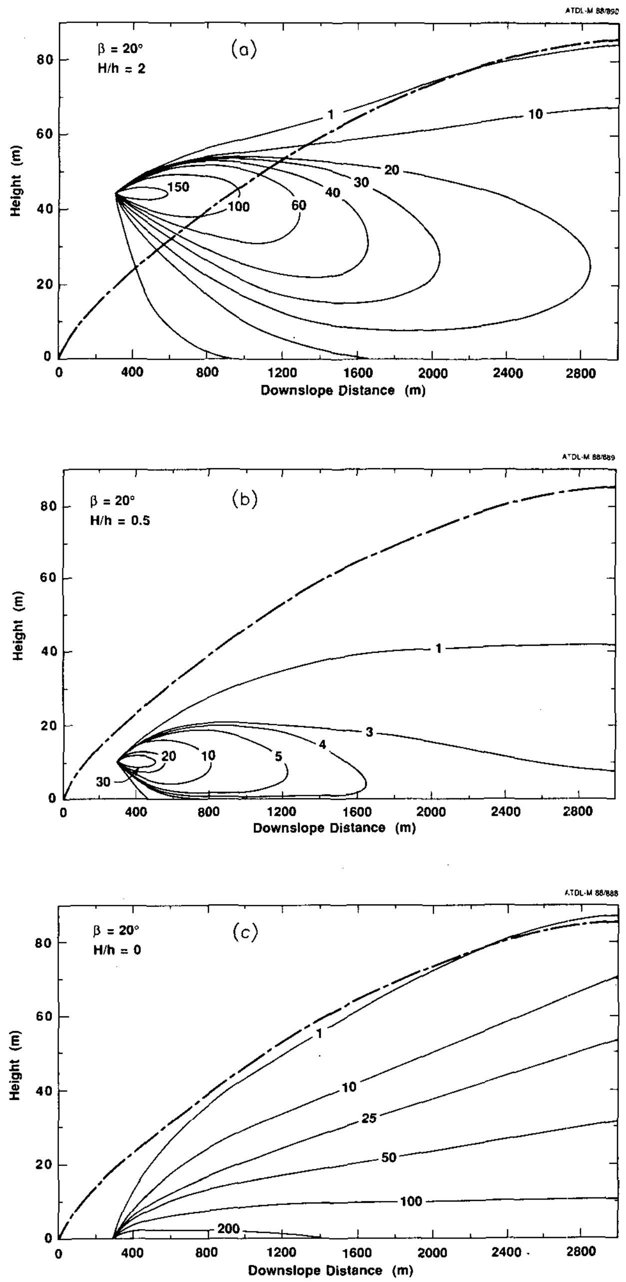

FIG. 4. Same as Fig. 3, but for the 20° slope.

Unauthenticated | Downloaded 05/21/24 07:09 AM UTC

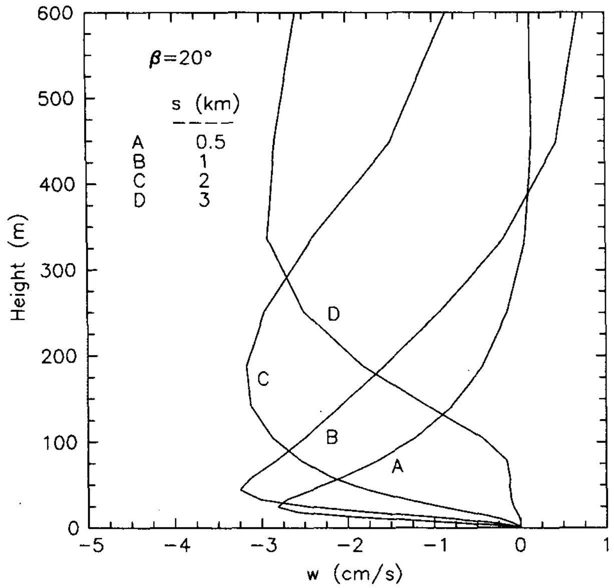

FIG. 5. Profiles of vertical velocity, w, at several downslope distances, s, in the katabatic flow over the 20° slope.

4. Tracer simulation

The applicability of this two-dimensional model to general terrain is demonstrated by simulating the perfluorocarbon and heavy methane tracer data of Night 4, 19/20 September, of the 1980 ASCOT field study in Anderson Creek Valley in the Geysers area of northern California. The purpose of these experiments, which included the simultaneous releases of four different tracers at different heights and locations, was to study the pollutant transport and diffusion within and above the drainage flow in the valley; they were not designed especially to test this model. Details and data for these experiments are given by Gudiksen (1983). Briefly, the night was clear with 5 m s^{-1} winds at the 850 mb level blowing from 355°. At the slope crest, northwesterly winds (290°–340°) prevailed throughout the night. Maximum winds varied from 3 to 6.5 m s^{-1}. Surface cooling rates increased from 0.8°C/h at the release site to about 1.5°C/h near sampling station S-4 (shown in Fig. 6b). The average drainage layer depth varied from 144 m near the release site to about 270 m at site S-4.

The topography of the valley is depicted in Fig. 6a. The valley is somewhat bowl-shaped; but the SE-facing slope of Cobb Mountain, along which Gunning and Anderson creeks run, is approximately two-dimensional. One of the perfluorocarbon tracers (PMCH, C_7F_{14}) was released into the Anderson Creek drainage, and another perfluorocarbon (PDCH, C_8F_{16}) was released into the Gunning Creek drainage; both tracers were released 5 m AGL. Two heavy methane tracer gases were released simultaneously but at different heights at the same location in the upper portion of Anderson Creek. Methane-21 was released 4 m AGL, and methane-20 was released between 60 m and 75 m AGL. All releases were between 2300 and 2400 PST; the amounts of materials released were: 1.27 g methane-21, 9.24 g methane-20, 416 g PMCH, and 471 g PDCH. The locations of the tracer release sites are shown in Fig. 6b.

We limit our comparisons between model predictions and observations to stations near the creeks, which we take to be the plume axes ($y = 0$). The locations of these stations are shown in Fig. 6b. The sampling times for the tracers at the various sampling sites are listed in Table 1. Because the model calculates dispersion from an infinite cross-wind line source, model results must be adjusted to account for cross-wind dispersion so that they can be compared with the observations. This is done by dividing the predicted concentrations by $(2\pi)^{1/2}\sigma_y$, where σ_y is taken from the Briggs curves for class B stability over open country (Hanna et al. 1982). Use of class B stability is based on the observed horizontal dispersion of constant volume balloons released over Anderson Creek during these experiments (Dickerson and Gudiksen 1983).

For these simulations, the following model input parameters were used: average slope angle of 15°, ambient wind speed of 4 m s^{-1} downslope, ambient thermal stratification of 12°C km^{-1}, surface roughness of 1 m, total cooling of the ground surface of 2°C, perfluorocarbon release sites located 2400 m from the crest of Cobb Mountain, and heavy methane release site located 1300 m from the crest. The model domain was extended to 7000 m by increasing the number of horizontal grid points to 71. The computational time step size was 6 seconds. The model takes about 5 CPU minutes on a CRAY X-MP computer for a 9 hour simulation.

Time series of predicted and observed perfluorocarbons at the sequential sampler sites are plotted in Figs. 7 and 8. Similar plots for heavy methanes are shown in Figs. 9 and 10. In all cases, the onset, buildup, and decay of concentration is predicted to occur sooner than was observed, which suggests that the drainage winds are overpredicted. The tendency for observed pollutant concentrations to decrease slowly or even to remain relatively constant throughout the night is attributed to the pooling of drainage air in the valley basin.

This pooling occurs due to the region of constricted outflow through a fairly narrow pass east of the confluence of Anderson, Gunning, and Putah creeks (Hosker et al. 1980). The pool of cold air backs up into the lower portions of the Anderson and Gunning creeks. The drainage speed decreases significantly as it encounters this pooling region, and pollutant concentrations build up because of the flow stagnation. This process could not be simulated in our two-dimensional model, which calculates the unrestricted flow down the slope. Model concentrations are, therefore, generally

Unauthenticated | Downloaded 05/21/24 07:09 AM UTC

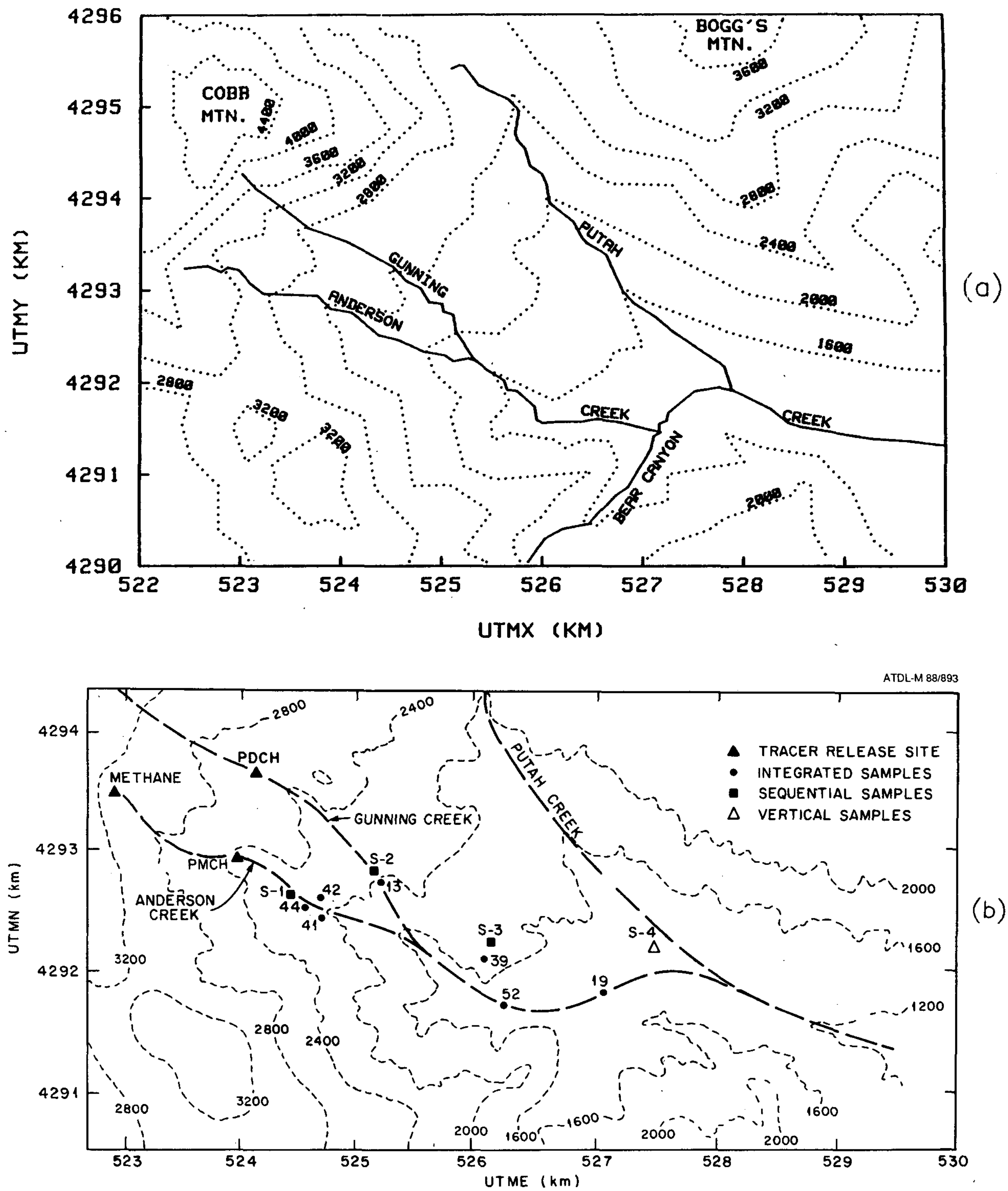

FIG. 6. (a) Topography of the Anderson Creek Valley, site of the 1980 ASCOT field study, in the Geysers area of northern California. The dotted lines show the elevation (MSL) contours in feet. (b) Locations of the perfluorocarbon and heavy methane tracer release sites and the sampler sites used in the present study.

smaller than those observed, except at station S-3 for the perfluorocarbons, Figs. 7b and 8b, and at station S-4 for the methane-20, Fig. 9b. Station S-3 is located about 450 m away from the creek horizontally and about 110 m above it vertically; because the model assumes that the receptors are located along the plume

Unauthenticated | Downloaded 05/21/24 07:09 AM UTC

TABLE 1. Sampling time for selected sequential and integrated samplers.

PMCH		PDCH		M-21 & M-20	
Site	Time (min)	Site	Time (min)	Site	Time (min)
19	120	13	120	39	480
44	120	19	120	41	480
52	120	52	120	42	480
S-1	10	S-2	15	52	480
S-3	15	S-3	15	S-1	30
S-4	20	S-4	20	S-4	30

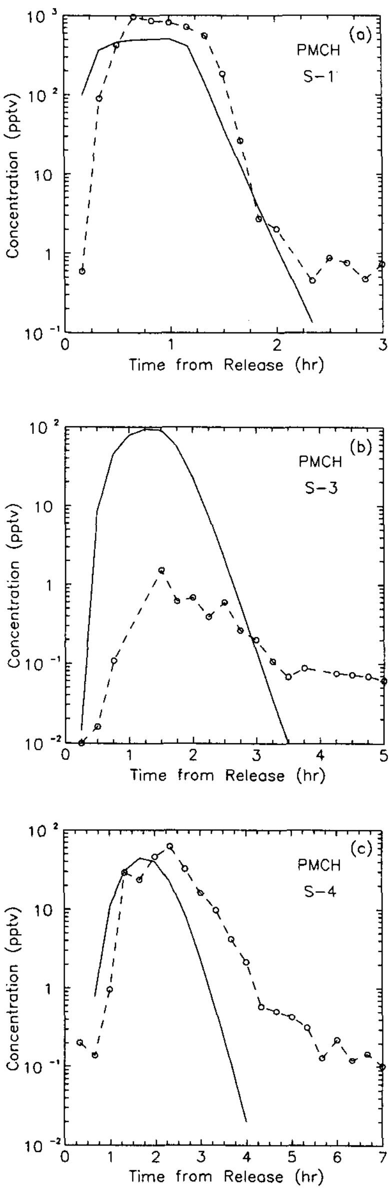

FIG. 7. Comparison of predicted (solid line) and observed (dashed line) PMCH concentrations, as a function of time from release, at the sequential sampler sites: (a) S-1, (b) S-3, and (c) S-4.

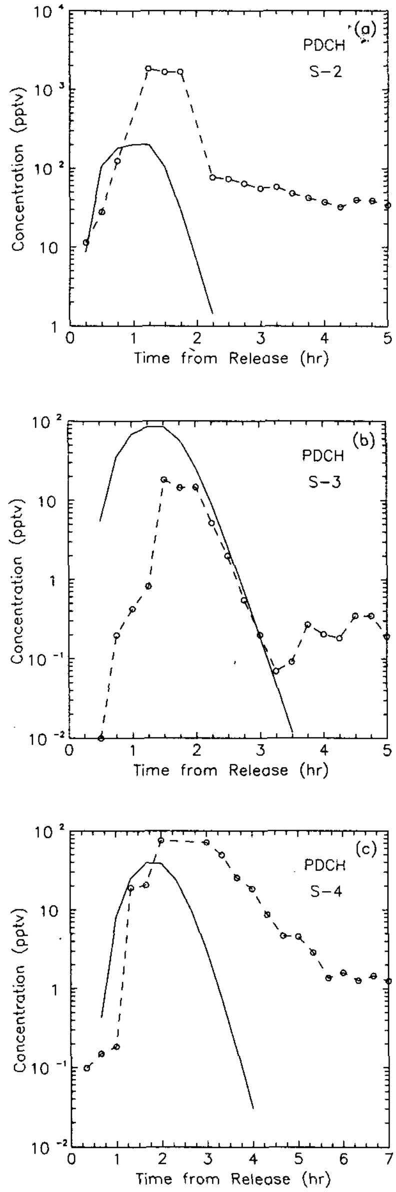

FIG. 8. Comparison of predicted (solid line) and observed (dashed line) PDCH concentrations, as a function of time from release, at the sequential sampler sites: (a) S-2, (b) S-3, and (c) S-4.

centerline at ground level, the concentrations at S-3 are overpredicted. The methane-20 tracer overprediction at S-4 is also due to similar reasons.

This behavior is further illustrated in Fig. 11, where the time-averaged vertical profile of the PMCH concentrations predicted at station S-4 is compared with the corresponding observed concentrations. Near the ground, the model performs well. Above the drainage layer, however, the model predicts a rapid decrease of pollutants with height. The stagnation of drainage air in the pooling region results in a very gradual decrease of observed concentrations with height. The overall

Unauthenticated | Downloaded 05/21/24 07:09 AM UTC

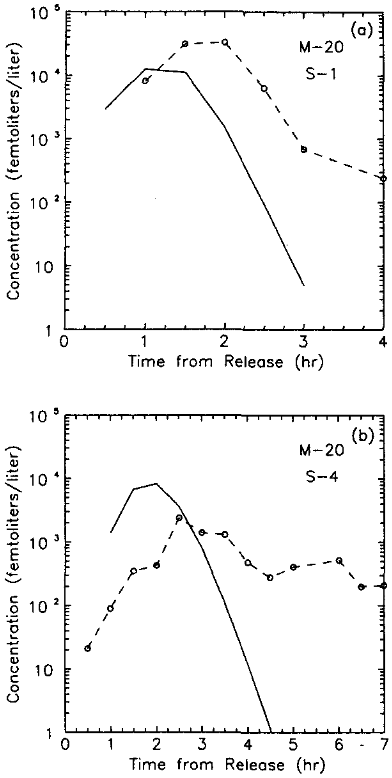

FIG. 9. Comparison of predicted (solid line) and observed (dashed line) methane-20 concentrations, as a function of time from release, at the sequential sampler sites: (a) S-1, and (b) S-4.

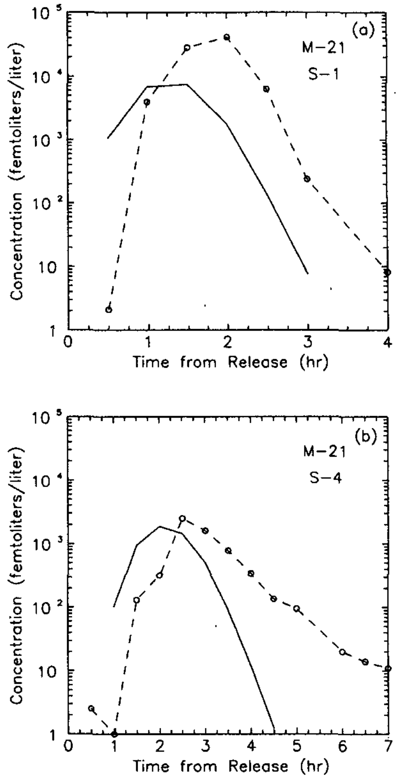

FIG. 10. Same as Fig. 9, but for methane-21 concentrations.

nighttime (i.e., 6-hour) averages of the predicted and observed perfluorocarbon concentrations at the integrated samplers are presented in Table 2. Except for station 13, these values are in good agreement, with an average value of the ratio of predicted to observed concentrations of 0.88.

The good results of these simulations clearly demonstrate the benefits of modeling the dynamics of katabatic flows. The species conservation equation (1) is quite general, and is the starting point for many modeling efforts; the success of this model is due to the physically realistic predictions of the wind and turbulence fields. Models which require the input of wind data are subject to the quality, quantity, and representativeness of these data, and they are not capable of generating a turbulence field consistent with the thermal stratification in the katabatic layer. For practical applications, this dynamic transport model requires a supercomputer; such machines are becoming rather commonplace, and should be even more accessible in the near future.

5. Conclusions

The ATDD two-dimensional katabatic flow model has been extended to include transport and diffusion. Using this model, we have examined the effects of source height and slope angle on dispersion in a simple drainage flow. Pollutants released above the drainage layer can be entrained into the layer and rapidly

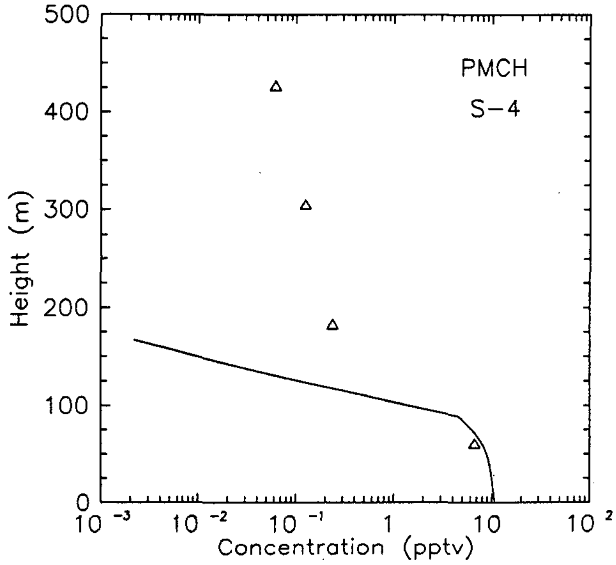

FIG. 11. Vertical profile of predicted (solid line) 6-h average concentration of PMCH at site S-4. Observations are indicated by triangles.

Unauthenticated | Downloaded 05/21/24 07:09 AM UTC

TABLE 2. Comparison of predicted and observed values of perfluorocarbon concentrations (in pptv) for selected integrated samplers.

Sampler site	Predicted	Observed
PMCH		
44	67	101
52	14	9
19	11	6
PDCH		
13	32	745
52	13	24
19	10	18

brought down to the ground surface. Pollutants released in the middle of the layer are transported downslope by the drainage wind, resulting in low concentrations at stack heights. In this case, subsidence in the flow leads to relatively high surface concentrations of pollutants close to the stack, especially on a shallow slope. Pollutants released at ground-level can spread through the entire depth of the drainage layer; this vertical diffusion is more effective for a shallow slope, and results in higher concentrations at all heights, than for a steeper slope. Thus, the characteristics of dispersion in drainage flows are different from those in the SBL over flat terrain. These differences are due to increases of wind speed, turbulence, and boundary-layer depth with downslope distance in the katabatic flow.

The applicability of this model to general slopes was tested by simulating the concentration data from several tracer releases in the 1980 ASCOT field study on a nearly two-dimensional slope in the Anderson Creek Valley. Calculated concentrations are generally smaller than those observed at sequential samplers located at ground-level along the creeks. The model could not account for the pooling of drainage air at the base of the slope, and the retardation of the downslope winds by this pooling. Because of this, the winds are overpredicted and the drainage layer depth is underpredicted near the bottom of the slope. This results in tracers being advected downslope more rapidly than was observed, but the average nighttime concentrations observed at the integrated samplers are predicted well. This model is most applicable for estimating steady state, ground level concentrations of pollutants released above and within drainage flows over nearly two-dimensional slopes. The model should be especially useful because it predicts concentrations without having to specify the winds and eddy diffusivities, requiring instead the input of easily estimated parameters.

Acknowledgments. This work was performed under an interagency agreement between the National Oceanic and Atmospheric Administration and the U.S. Department of Energy as part of the ASCOT program.

REFERENCES

Briggs, G. A., 1981: Canopy effects on predicted drainage flow characteristics and comparisons with observations. *Proc. Fifth Symposium On Turbulence and Diffusion,* Atlanta, Amer. Meteor. Soc., 113–115.

Businger, J. A., J. C. Wyngaard, Y. Izumi and E. F. Bradley, 1971: Flux-profile relations in the atmospheric surface layer. *J. Atmos. Sci.,* **28,** 181–189.

Dickerson, M. H., and P. H. Gudiksen, 1983: Atmospheric studies in complex terrain technical progress report FY-1979 through FY-1983. Lawrence Livermore National Lab., UCID-19851, ASCOT-84-1, 376 pp.

Ellison, T. H., and J. S. Turner, 1959: Turbulent entrainment in stratified flows. *J. Fluid Mech.,* **6,** 423–448.

Gudiksen, P. H., 1983: ASCOT data from the 1980 field measurement program in the Anderson Creek Valley, California. Lawrence Livermore National Lab., UCID-18874-80, ASCOT-83-1, 1202–1316.

Hanna, S. R., G. A. Briggs and R. P. Hosker, Jr., 1982: Handbook on atmospheric diffusion. DOE/TIC-11223 (DE82002045), National Technical Information Service, U.S. Dept. of Commerce, Springfield, VA, 102 pp.

Hosker, R. P., K. S. Rao and G. A. Briggs, 1980: Experimental methods and preliminary analyses of drainage flow observations during the first ASCOT field study. *Proc. Second Joint Conference on Applications of Air Pollution Meteorology and Second Conference on Industrial Meteorology,* New Orleans, LA, Amer. Meteor. Soc., 483–494.

King, J. A., F. H. Shair and D. D. Reible, 1987: The influence of atmospheric stability on pollutant transport by slope winds. *Atmos. Environ.,* **21,** 53–59.

Nappo, C. J., and K. S. Rao, 1987: A model study of pure katabatic flow. *Tellus,* **39A,** 61–71.

Rao, K. S., R. M. Eckman and R. P. Hosker, 1989: Simulation of tracer concentration data in the Brush Creek drainage flow using an integrated puff model. *J. Appl. Meteor.,* **28,** 609–616.

Willson, R., F. Shair, B. Reynolds and W. Greene, 1983: Characterization of the transport and dispersion of pollutants in a narrow mountain valley region by means of an atmospheric tracer. *Atmos. Environ.,* **17,** 1633–1647.

Unauthenticated | Downloaded 05/21/24 07:09 AM UTC